MOLECULAR AND CELLULAR BIOLOGY, Apr. 2007, p. 3056–3064 Vol. 27, No. 8
0270-7306/07/$08.00+0 doi:10.1128/MCB.01339-06

Rbm15 Modulates Notch-Induced Transcriptional Activation and Affects Myeloid Differentiation▽†

Xianyong Ma,[1]‡ Matthew J. Renda,[1]‡ Lin Wang,[1] Ee-chun Cheng,[1] Chao Niu,[2] Stephan W. Morris,[2] Andrew S. Chi,[1] and Diane S. Krause[1]*

Departments of Laboratory Medicine and Pathology, Yale University School of Medicine, New Haven, Connecticut,[1] and Departments of Pathology and Tumor Cell Biology at St. Jude Children's Research Hospital and Department of Pediatrics, University of Tennessee, College of Medicine, Memphis, Tennessee[2]

Received 20 July 2006/Returned for modification 12 September 2006/Accepted 22 January 2007

***RBM15* is the fusion partner with *MKL* in the t(1;22) translocation of acute megakaryoblastic leukemia. To understand the role of the RBM15-MKL1 fusion protein in leukemia, we must understand the normal functions of RBM15 and MKL. Here, we show a role for Rbm15 in myelopoiesis. Rbm15 is expressed at highest levels in hematopoietic stem cells and at more moderate levels during myelopoiesis of murine cell lines and primary murine cells. Decreasing Rbm15 levels with RNA interference enhances differentiation of the 32DWT18 myeloid precursor cell line. Conversely, enforced expression of Rbm15 inhibits 32DWT18 differentiation. We show that Rbm15 alters Notch-induced *HES1* promoter activity in a cell type-specific manner. Rbm15 inhibits Notch-induced *HES1* transcription in nonhematopoietic cells but stimulates this activity in hematopoietic cell lines, including 32DWT18 and human erythroleukemia cells. Moreover, the N terminus of Rbm15 coimmunoprecipitates with RBPJκ, a critical factor in Notch signaling, and the Rbm15 N terminus has a dominant negative effect, impairing activation of *HES1* promoter activity by full-length-Rbm15. Thus, Rbm15 is differentially expressed during hematopoiesis and may act to inhibit myeloid differentiation in hematopoietic cells via a mechanism that is mediated by stimulation of Notch signaling via RBPJκ.**

Acute megakaryoblastic leukemia (AML-M7, also referred to as AMKL) comprises approximately 10% of childhood AML, in which it frequently presents in infants with bone marrow fibrosis and progresses rapidly, with a median survival of 8 months. This phenotype is associated with the t(1;22)(p13; q13) translocation, which was first observed in several infants with AML-M7 (5) and subsequently confirmed by others to be associated almost exclusively with this type of AML (2, 30, 31, 34). The t(1;22) translocation has only very rarely been associated with the AML-M7 cases that occur in association with trisomy 21; in general, AML-M7 with trisomy 21 is nearly always associated with mutations in the GATA1 gene (14, 32). In t(1;22), the breakpoint on chromosome 1p13 is within a gene that has been variably named *RBM15* for RNA-binding motif protein 15 and *OTT* (for one twenty-two translocation), and the breakpoint on chromosome 22 is within the *MKL1* gene (also known as MAL or BSAC).

The *MKL1* gene product is a 4.5-kb transcript that is widely expressed in normal tissues (35) and encodes one of three members of the myocardin family. While these three members, i.e., MKL1, MKL2, and myocardin, are only 35% similar to one another at the protein level, they have several highly conserved domains, including RPEL repeats in the N terminus, a region with a B (basic amino acid) box and a glutamine-rich domain that is involved in binding to serum response factor, a leucine zipper-like domain that plays a role in homo- and heterodimerization, and a C-terminal transactivation domain. These proteins also have a SAP domain that, based on its homology to SAF-B, is predicted to associate with matrix attachment regions of transcriptionally active chromatin. Myocardin and the MKL proteins promote transcriptional activation of serum response factor-responsive genes, including both growth-related genes (e.g., c-*fos*) and differentiation-associated (nonproliferative) muscle-specific genes, in different cell types (27). In addition, MKL inhibits cell death in embryonic fibroblasts, which may be relevant to its role in AML-M7 (9).

The t(1;22) breakpoint on chromosome 1 is located within a 4-kb intron of the *RBM15* gene downstream of the exon encoding the C-terminal SPOC domain, and it generates an in-frame fusion with *MKL1* that contains nearly the full-length coding regions of both *RBM15* and *MKL1* with the predicted chimeric protein containing 1,833 amino acids (1, 15, 34). Although the biological function of RBM15 is not yet known, SHARP, another member of the spen family of proteins that is conserved from *Drosophila*, is associated with transcriptional repression and can inhibit Notch signaling by binding to RBPJκ (26, 38). In *Drosophila*, spen plays a role in inhibiting cell division and affects cell fate specification, survival, and axonal guidance via interactions with the Hox, E2F, Notch, and Ras/Raf signaling pathways (7, 25).

This report describes a potential role for Rbm15 in normal myelopoiesis. We show that Rbm15 is a nuclear protein that is differentially expressed during myelopoiesis. Suppression of Rbm15 facilitates myeloid differentiation, and enforced ex-

* Corresponding author. Mailing address: Yale University School of Medicine, Department of Laboratory Medicine, P.O. Box 208035, 333 Cedar Street, New Haven, CT 06520-8035. Phone: (203) 688-4829. Fax: (203) 688-2748. E-mail: diane.krause@yale.edu.

† Supplemental material for this article may be found at http://mcb.asm.org/.

‡ These authors contributed equally to the work.

▽ Published ahead of print on 5 February 2007.

pression inhibits differentiation. We find that Rbm15 can co-immunoprecipitate in the nucleus with RBPJκ, which suggests that its effects on myeloid differentiation may be mediated via RBPJκ.

MATERIALS AND METHODS

Cell cultures. Chinese hamster ovary (CHO) cells were grown in F12 medium (GIBCO/BRL, Rockville, MD) with 5% fetal calf serum, 2 mM glutamine, 50 units/ml penicillin, and 50 μg/ml streptomycin. EML cells were grown in Iscove modified Eagle medium with 20% horse serum, 15% BHK conditioned medium (as a source of stem cell factor), 0.1 mM nonessential amino acids, 2 mM glutamine, 50 units/ml penicillin, and 50 μg/ml streptomycin. EML cells were induced to differentiate with 10 μM all-*trans* retinoic acid, and interleukin-3 (IL-3) (10 ng/ml) for the indicated times. 32DWT18 cells (hereafter called WT18 cells; a gift from Daniel Link, Washington University, St. Louis, MO) were derived from 32D cells that were stably transfected with a chimeric receptor containing the extracellular domain of the erythropoietin receptor and the intracellular domain of the granulocyte colony-stimulating factor receptor. They were grown in Iscove's modified Dulbecco's medium, 10% fetal bovine serum, 10% WEHI-3B conditioned medium (as a source of IL-3), 2 mM glutamine, 50 units/ml penicillin, and 50 μg/ml streptomycin (22). WT18 cells were induced to differentiate into neutrophils by withdrawal of IL-3 and addition of 2 U/ml of erythropoietin (EPO). The retroviral packaging cell line PT67 was cultured in Dulbecco modified Eagle medium, 10% fetal calf serum, 2 mM glutamine, 50 units/ml penicillin, and 50 μg/ml streptomycin.

Cloning of mouse *Rbm15* cDNA and construction of its derivatives. Total RNA from EML cells was isolated using TRIzol reagent according to the manufacturer's instruction (Invitrogen). Primers for amplifying mouse *Rbm15* were Pf (5′ CCAATGAGGTCTGCGGGGCG) and Pr (5′CCTCAAAAGAAACAATTTA TTTAGAA). All *Rbm15* fragments and positions referred to in this paper correspond to DDBJ/EMBL/GenBank accession number BC057038. Reverse transcription-PCR (RT-PCR) was carried out following standard protocols. The full-length mouse *Rbm15* open reading frame was inserted into pNTGFP vector, yielding an expression construct, pNTGFP-*Rbm15*, containing an in-frame fusion of the green fluorescent protein (GFP) gene downstream from *Rbm15*. The *Rbm15* N-terminal (amino acids [aa] 1 to 608) truncated fragment was inserted into pcDNA3HA vector to generate HA-*N*/*Rbm15*, and the C-terminal (aa 635 to 962) truncated fragment was inserted into pcDNA3*myc* vector to generate *myc-C*/*Rbm15*. The shorter truncated fragments for N-terminal *V-Rbm15-F1* (aa 1 to 453), *V-Rbm15-F2* (aa 1 to 355), *V-Rbm15-F3* (aa 1 to 306), and *V-Rbm15-F4* (aa 1 to 198) were generated by insertion of the fragments into the pcDNA3V5 TOPO cloning vector. Mouse *RbpJκ* expression vector pcDNA3Flag-RBPJκ was previously described (29).

Northern blot analysis. For Northern blot analysis, 12 μg total RNA was run on a 1% agarose–0.6% formaldehyde gel, transferred to a Hybond-N (Amersham Inc., Piscataway, NJ) membrane, and hybridized according to the supplier's protocol. The probe for *Rbm15* mRNA detection encompassed the full-length open reading frame. A murine multitissue RNA blot was purchased from Clontech.

Real-time RT-PCR to detect *Rbm15* expression in hematopoietic cells. Total RNA was isolated from 1×10^6 cells using the Roche High Pure RNA isolation kit. Two micrograms of total RNA was reverse transcribed with Superscript II RNase H^- reverse transcriptase (Invitrogen) and 100 ng of random hexamers. Real-time PCR analysis was performed with a Bio-Rad iCycler using the iQSYBER green supermix (Bio-Rad) for murine GAPDH (glyceraldehyde-3-phosphate dehydrogenase) internal control (forward primer, 5′GGTGAAGGT CGGTGTGAA; reverse primer, 5′AATGAAGGGGTCGTTGATG). We used Applied Biosystems TaqMan Gene Expression Assays Mm01207208 and the default cycles for detecting the murine *Rbm15*. Standard curves for *Gapdh* and *Rbm15* were measured each time to determine the relative level of the respective transcript. The copy number was normalized to *Gapdh* levels.

Immunoprecipitation and Western blot analysis. Antibodies against GFP and RBPJκ, as well as anti-GFP-conjugated beads were purchased from Santa Cruz Inc. CHO cells were transfected with plasmids and 24 h later were washed and scraped into 5 ml of phosphate-buffered saline, centrifuged, and resuspended in 3 packed cell volumes of Triton lysis buffer (9 mM Tris-HCl [pH 8.0], 60 mM EDTA, 1 mM dithiothreitol [DTT], 0.5 mM phenylmethylsulfonyl fluoride, and 0.3% Triton X-100). After 5 min on ice, the lysates were sedimented by centrifugation, and the supernatant was used as the cytoplasmic extract. The pelleted nuclei were washed, and nuclear proteins were extracted with 2 packed cell volumes of nuclear extract buffer (20 mM HEPES [pH 8.0], 420 mM NaCl, 1.5 mM $MgCl_2$, 0.5 mM DTT, 0.2 mM EDTA, and 25% glycerol) at 4°C for 45 min. Soluble material was pelleted, and the supernatant was dialyzed at 4°C for 1 h against Shapiro's buffer D (20 mM HEPES [pH 7.9], 20% glycerol, 100 mM KCl, 2 mM DTT, 0.2 mM EDTA, 0.2 mM EGTA, 0.5 mM phenylmethylsulfonyl fluoride, 0.7 mg/liter pepstatin A, and 0.5 mg/liter leupeptin). The precipitate was removed by centrifugation, and the supernatant fraction was the nuclear extract. The nuclear extract was then precleared with 0.25 μg of the appropriate control immunoglobulin G (goat immunoglobulin G; anti-GFP was from goat) together with 20 μl of protein L-agarose and incubated at 4°C for 30 min, beads were pelleted by centrifugation, and the supernatant was then mixed with anti-GFP beads and incubated at 4°C with rotation for at least 3 h. The beads were then washed and collected by centrifugation. The protein bound to the beads was eluted with sample loading buffer, boiled for 5 min, analyzed by sodium dodecyl sulfate-polyacrylamide gel electrophoresis and immunoblotting, and visualized using the ECL system (Amersham Biosciences). Anti-Flag M2 affinity gels were purchased from Sigma. Antihemagglutinin (anti-HA) antibody and anti-myc antibody were purchased from Santa Cruz Biotechnology Corp. The anti-V5 antibody and pcDNA3-V5-His-TOPO vector were purchased from Invitrogen Corp.

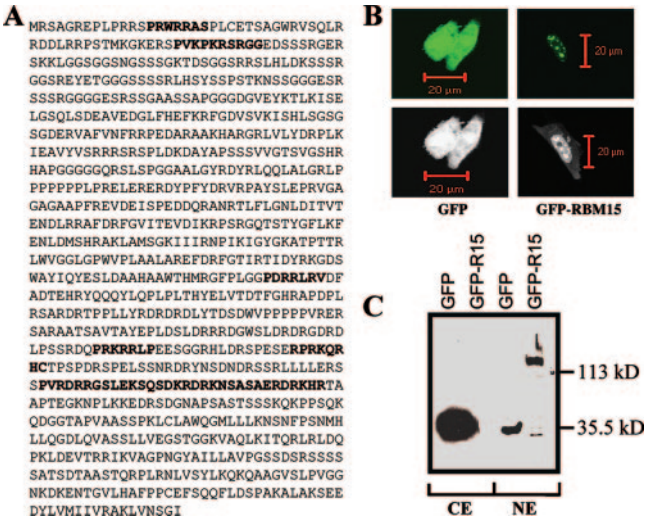

FIG. 1. Mouse RBM15 protein sequence and subcellular localization. (A) Full-length mouse Rbm15 protein sequence, with predicted nuclear localization signals shown in boldface. (B) CHO cells were transfected with plasmids encoding GFP (left) or GFP-Rbm15 (right) proteins. The upper panels show Rbm15 subcellular localization (right) (based on GFP fluorescence) by confocal microscopy at 24 h posttransfection. Images in the lower panels reveal the autofluorescence of the cells above. (C) Western blot analysis of CHO cells transiently transfected with plasmid encoding GFP or GFP-Rbm15. Cytoplasmic extract (CE) and nuclear extract (NE) were derived from the CHO cells, and the transgenes (as indicated above each lane) were detected with anti-GFP. Numbers at right represent relative locations of molecular mass standards.

Microscopy and flow cytometry. CHO cells in two-well chamber slides were transfected with 0.5 μg total of pNTGFP-*Rbm15* or pNTGFP expression plasmids using Lipofectamine 2000 (Invitrogen) according to the manufacturer's protocol. After 24 h, the fluorescence of transfected cells was detected by confocal microscopy to show the subcellular localization of RBM15 protein. For fluorescence-activated cell sorter (FACS) analysis, cells were stained with fluorescein isothiocyanate-conjugated anti-Mac-1 (CD11b) antibody (BD Biosciences), washed three times, and analyzed using a FACSCalibur (BD Biosciences).

Construction and packaging of shRNA vectors. The four following *Rbm15*-specific small hairpin RNA (shRNA) oligomers were tested: 5′GATCCGAGGAA CCTTGTGTCCTATTTAAATTCAAGAGATTTAAATAGGACACAAGGTTC CTTTTTTACGCGT (shRNA-Oligo I, corresponding to nucleotides 2668 to 2689), 5′GATCCGACTCTGCTATTGTGATGCCAATGTTCAAGAGACATTGGCA TCACAATAGCAGATTTTTTTACGCGT (shRNA-Oligo II, corresponding to nucleotides 3028 to 3049), 5′GATCCGACCGAGACTATCCGTTCTATGACTT

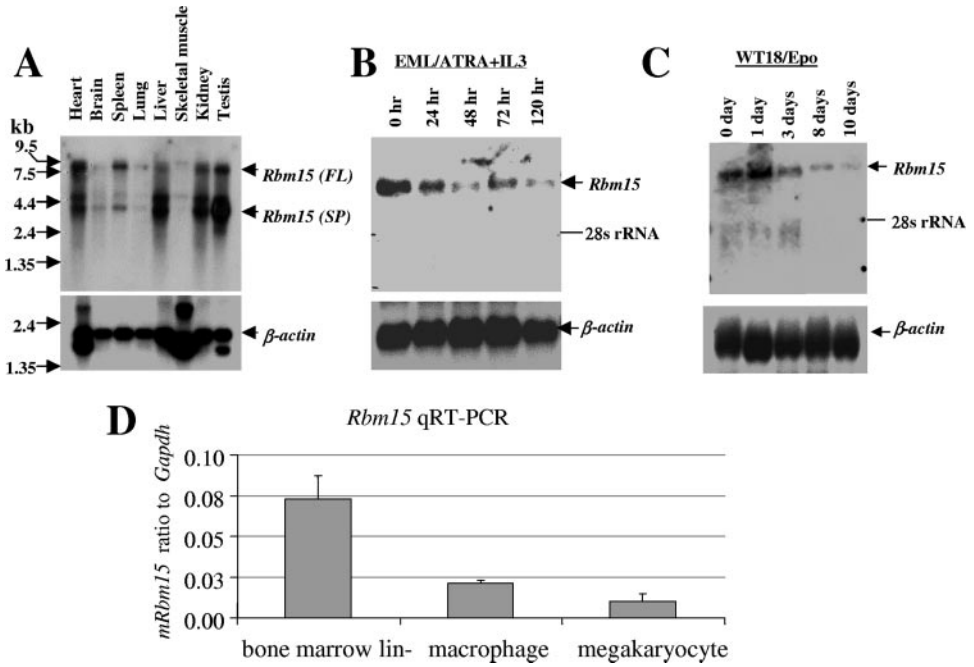

FIG. 2. *Rbm15* expression in tissues and myeloid cells. (A to C) Analysis of *Rbm15* using a murine multitissue Northern blot (A), as well as during myeloid differentiation of EML (B) and 32DWT18 cells (C). β-Actin mRNA was probed as a loading control (bottom). Note that two forms of *Rbm15* predominate, one at approximately 9 kb (full length [FL]) and the other at 4 kb (spliced [SP]) in the tissues but not in the myeloid cell lines. (D) qRT-PCR data for Rbm15 in primary lineage-negative murine bone marrow cells, as well as in macrophages and megakaryocytes differentiated from primary bone marrow. Error bars indicate standard deviations.

CAAGAGAGTCATAGAACGGATAGTCTCGTTTTTTTACGCGT (shRNA-Oligo III, corresponding to nucleotides 986 to 1007), and 5′GATCCGACTCCGAGAAGTGGATGAGATATTTCAAGAGAATATCTCATCCACTTCTCGGAATTTTTTACGCGT (shRNA-Oligo IV, corresponding to nucleotides 1068 to 1089). Sequences corresponding to the target-specific small interfering RNA duplex are underlined, and target nucleotide sequences are shown in parentheses. Sense and antisense oligomers were used to produce double-stranded oligomers, and the oligomers were inserted into the retroviral vector RNAi-pSIREN-RetroQ, which drives shRNA production from the U6 promoter and also contains puromycin resistance (Clontech, Palo Alto, CA). Inserts were confirmed by sequencing, and we called the vectors shRNA-I, shRNA-II, shRNA-III, and shRNA-IV, respectively. Retroviral constructs were transiently transfected into PT67 amphotropic packaging cells using Lipofectamine 2000 (Invitrogen), and the viral supernatants were collected at 24 to 48 h after transfection and stored at −80°C for future use.

Retroviral infection and cell proliferation assay. 32DWT18 cells were plated 24 h before infection at 1×10^6 to 5×10^6/100-mm dish. Viral supernatants containing shRNA-negative, shRNA-III, or shRNA-IV retrovirus were added individually at a 1:2 dilution to medium supplemented with WEHI conditioned medium (containing IL-3) and 6-μg/ml Polybrene. After 24 h, fresh medium containing 2 μg/ml of puromycin was added, and cells were cultured for 3 days. After 3 days, surviving cells, i.e., those containing puromycin-resistant/shRNA retrovirus, were induced to undergo myeloid differentiation by the withdrawal of IL-3 and addition of EPO. Proliferation was measured by counting the number of cells per culture well at 3 and 6 days postinduction. To study the effects of enforced expression of RBM15, WT18 cells were transduced with retrovirus encoding the Rbm15 protein or empty vector. Cells were then induced to differentiate with EPO, and differentiation was assayed by cell morphology and surface expression of Mac1 by flow cytometry.

Transient transfection and luciferase assays. Luciferase assays were performed using the dual luciferase reporter system (Promega, Madison WI). Briefly, 5×10^4 CHO cells were seeded in 12-well plates and cotransfected with 0.5 μg of Hes-Luc reporter gene, 0.1 μg of the intracellular domain of Notch (NICD), 2 ng of pRL-CMV-Rluc (for normalization), and various amounts of *Rbm15* plasmid (0.01 to 0.95 μg) using Lipofectamine 2000. For experiments with human erythroleukemia (HEL) cells, 1×10^6 cells were seeded in 12 well plates and cotransfected with 0.5 μg of Hes-Luc reporter gene, 0.1 μg of NICD, 5 ng of pRL-CMV-Rluc, and various amounts (0.1 to 0.5 μg) of *Rbm15* plasmid (or empty vector), using the DMRIE-C reagent according to the manufacturer's instructions (Invitrogen). The total DNA content was kept at 2 μg with the use of empty plasmid pCDNA3.1 (Invitrogen, Carlsbad CA). For experiments with 32DWT18 cells, 1×10^7 cells were electroporated (400 V, 250 μF; Bio-Rad) with 5 μg Hes-Luc, 1 μg of NICD, 0.5 μg of pRL-CMV-Rluc (*Renilla* luciferase), and various amounts (1 to 10 μg) of the *Rbm15* plasmid. The total DNA content was kept at 20 μg using empty pCDNA3.1 plasmid. After 24 h, the transfected cells were washed and lysed with passive lysis buffer (Promega), and luciferase activity was measured using a Luminoscan EL (Thermo Electron) luminometer. Firefly luciferase activity from Hes-Luc was normalized for transfection efficiency using *Renilla* luciferase activity from pRL-CMV-Rluc. All experiments were performed in triplicate, and each study was performed at least three times.

Alignments. The evolutionary distance for the SPOC domain of different spen family members was determined by using ClustaIW software from the European Molecular Biological Laboratory-European Bioinformatics Institute (EMBL-EBI), and the phylogenetic tree was generated to show the relationships between RBM15 and other members.

RESULTS

Rbm15 is localized to the nucleus. Based on the presence of several potential nuclear localization signals in its amino acid sequence (Fig. 1A), we predicted that Rbm15 is a nuclear protein. To determine the subcellular localization of Rbm15, we transiently expressed either GFP (Fig. 1B, left panels) or a GFP-Rbm15 fusion protein (Fig. 1B, right panels) in CHO cells. After 24 h, cells were analyzed for GFP localization. In cells transfected with GFP-Rbm15, the GFP signal was localized to the nucleus (Fig. 1B, right panels). Analysis of autofluorescence (Fig. 1B, lower panels), confirmed that the cytoplasm was intact and negative for the GFP-Rbm15 fusion protein. In contrast, there was fluorescence throughout the cytoplasm and

nucleus in cells transfected with GFP cDNA (Fig. 1B, left panels). This subcellular localization was confirmed by Western blot analysis for GFP or GFP-Rbm15 in isolated cytoplasmic and nuclear fractions of CHO cells. As shown in Fig. 1C, the 133-kDa GFP-Rbm15 fusion protein was found exclusively in the nuclear extract, whereas the 35-kDa GFP protein was present in both the cytoplasmic and nuclear extracts.

Rbm15 is differentially expressed during hematopoiesis. By Northern blot analysis of a murine multitissue RNA blot, *Rbm15* is expressed at variable levels throughout the body, with the highest levels of expression in adult heart, liver, kidney, and testis (Fig. 2A). As reported previously (31), two splice variants of *Rbm15* mRNA are prominent, with the larger form reflecting the presence of a long 3′ untranslated sequence. We next determined whether *Rbm15* mRNA levels change during myeloid differentiation. As can be seen in Fig. 2B and C, *Rbm15* levels steadily decline when EML and 32DWT18 cells differentiate into promyelocytes and more mature neutrophils. Likewise, based on quantitative RT-PCR, the relative levels of *Rbm15* in primary murine bone marrow cell subpopulations are highest in lineage-depleted bone marrow cells, with less expression in differentiated macrophages and megakaryocytes (Fig. 2D).

Development of shRNA vectors to decrease Rbm15 expression. In order to determine the effect of decreasing Rbm15 levels on hematopoiesis, we produced several shRNA sequences targeted to different regions of the *Rbm15* mRNA (Fig. 3A) and cloned each into a retroviral vectors. We tested the efficacy of each sequence by cotransfecting the shRNA retroviral constructs along with *GFP-Rbm15* and looked for knockdown of the fusion by Western blotting. Whereas shRNA-I had a minimal effect on the amount of GFP-Rbm15 protein produced, shRNA-II, -III, and -IV sequences caused a nearly 100% decrease in GFP-Rbm15 protein (Fig. 3B). A control shRNA against luciferase had no effect on GFP-Rbm15 expression (Fig. 3B). We confirmed shRNA efficacy by observing a loss of GFP fluorescence by FACS when cells were cotransfected with the *GFP-Rbm15* vector plus Rbm15-specific shRNA vector (data not shown). Based on our findings, we chose to perform further studies with shRNA-III and shRNA-IV. To first test the effect of shRNA against *Rbm15* on proliferation of myeloid cells, 32DWT18 cells were transduced with retroviruses encoding shRNA-III, shRNA-IV, or the negative control shRNA. Both shRNA-III and shRNA-IV slowed the growth of WT18 cells by 80 to 90% (Fig. 3C). Therefore, Rbm15 may play a role in promoting proliferation of myeloid progenitors.

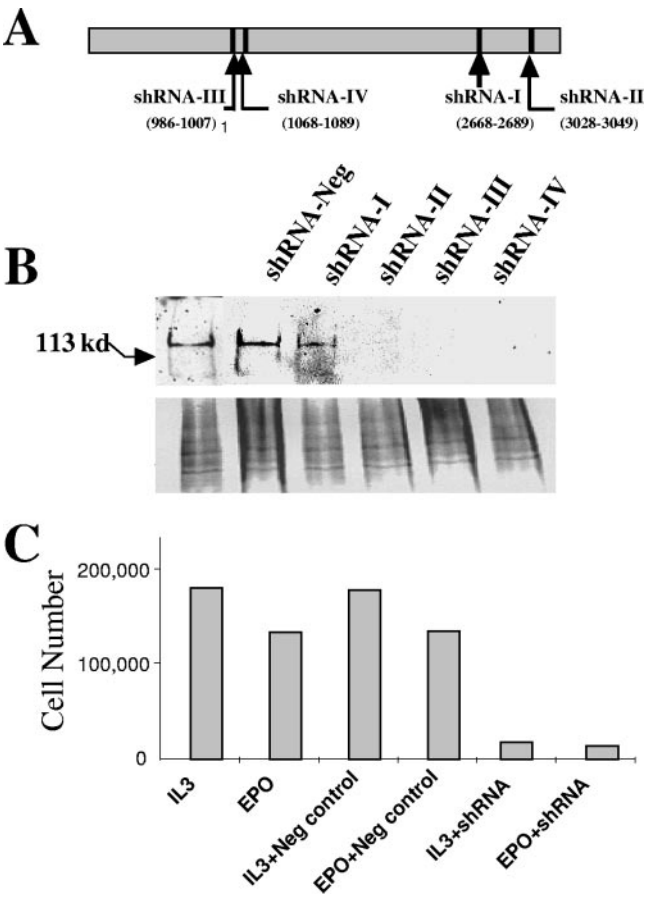

FIG. 3. Targeted inhibition of Rbm15 expression by RNA interference. (A) Schematic showing locations of four shRNAs tested for inhibition of Rbm15 expression. (B) Transient cotransfection of CHO cells using a GFP-Rbm15 expression plasmid together with shRNA-I, shRNA-II, shRNA-III, shRNA-IV, or negative control (luciferase shRNA) retroviral constructs separately. After transfection, nuclear lysates were analyzed for GFP-Rbm15 expression by Western blot analysis using anti-GFP antibody. The upper panel shows the GFP-Rbm15-specific band, and the lower panel shows the protein loading (Coomassie blue stain) for the blot. (C) Relative cell numbers of 32DWT18 cells transduced with retroviruses and cultured in the presence of growth factors as indicated on the *x* axis. Cell counts were assessed after 6 days of culture. The shRNA-IV vector was used in the experiment shown.

Small inhibitory RNA against Rbm15 promotes myeloid differentiation. We next assessed the effect of *Rbm15* knockdown on myeloid differentiation by morphological and FACS analyses. When transduced with negative control shRNA retrovirus, 32DWT18 cells began to undergo morphological differentiation into metamyelocytes by day 4 of EPO induction (Fig. 4A and B). In contrast, cells transduced with shRNA-III or shRNA-IV were further along in differentiation by this time point, with the appearance of bands and maturing neutrophils (Fig. 4C and D). FACS analysis for Mac1 expression demonstrated that cells transduced with shRNA-III also showed a more rapid onset of Mac 1 expression than those transduced with the negative control shRNA (Fig. 4E and F). Both shRNA-III and shRNA-IV (not shown) caused a 30 to 50% increase in Mac 1 expression at days 4 and 6. By day 10, however, all cells were Mac1 positive, including those that had been transduced with the negative control shRNA (Fig. 4G). The increase in myeloid differentiation with shRNA against Rbm15 is consistent with the observed decrease in cell proliferation.

Enforced expression of Rbm15 inhibits myeloid differentiation. Consistent with the enhancement of differentiation by shRNA, enforced expression of Rbm15 in 32DWT18 cells via retroviral transduction inhibits differentiation. As seen in Fig. 4H, the percentage of cells expressing Mac1 is significantly decreased throughout the time course of myeloid differentiation in the Rbm15-overexpressing cells compared to control cells transduced with empty control vector MigR1. Taken together, these data suggest that Rbm15 promotes cell proliferation and inhibits myeloid differentiation.

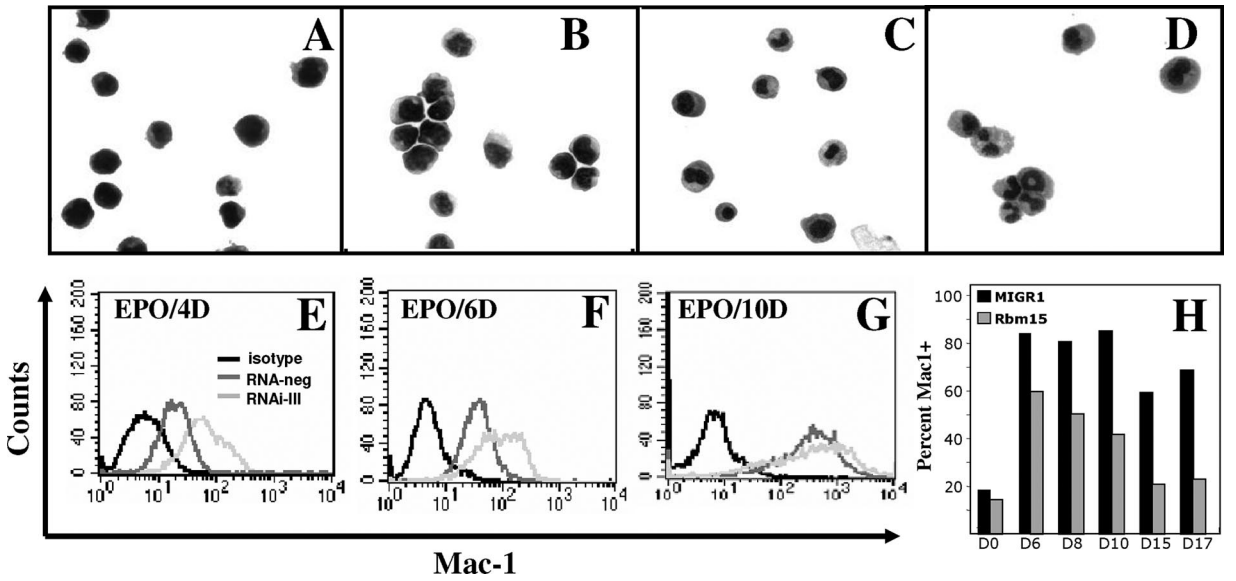

FIG. 4. Altered Rbm15 expression affects myeloid differentiation of 32DWT18 cells. 32DWT18 cells were induced to undergo myeloid differentiation by removal of IL-3 and addition of EPO. (A to D) Wright-Giemsa-stained cytospins of day 0 cells (A) and cells on day 4 postdifferentiation transduced with negative control shRNA (B), shRNA-III (C), or shRNA-IV (D). (E to G) FACS analysis histograms using anti-CD11b (Mac1) for 32DWT18 cells transduced with either the negative control shRNA (dark gray) or shRNA-III (light gray) as indicated and then treated with EPO for 4, 6, and 10 days, as indicated. The isotype control (black line) was identical for cells transduced with negative control shRNA or shRNA-III. Untransduced controls gave staining identical to that for shRNA-negative cells (not shown). (H) Percentage of 32DWT18 cells that were $Mac1^+$ (*y* axis) at different days after EPO induction (*x* axis) for cells transduced with control retrovirus (MIGR1, black lines) or Rbm15-encoding retrovirus (gray lines). Data are representative of two experiments.

Rbm15 is a member of the spen family. Rbm15 contains a C-terminal SPOC domain (spen paralog and ortholog C-terminal domain), which has been conserved from the *Drosophila* spen (derived from split ends) gene (see Fig. S1 in the supplemental material). The mammalian SPOC family protein most closely related to Rbm15 is SHARP (the murine homolog of which is called Mint), which has been shown to act as a transcriptional repressor by binding to proteins in the nuclear corepressor complex, including histone deacetylase 1, histone deacetylase 3, and SMRT (45, 47). The SPOC domain of Rbm15 is 35% homologous to SHARP. Published experimental data demonstrating a transcriptional repressor function for SHARP suggest that Rbm15 may act as a transcriptional repressor. Also, evolutionary tree analysis (see Fig. S1 in the supplemental material) indicates that Spen2 and Spen3 are more similar to human SHARP and mouse Mint than Spen1.

Effect of Rbm15 on transcription is cell type dependent. We first tested whether Rbm15 acts as a transcriptional repressor by using luciferase assays with CHO cells. Neither GFP nor GFP-Rbm15 had any effect on luciferase expression driven by the cytomegalovirus promoter (Fig. 5A). We next determined whether Rbm15 affects Notch-induced activation of the *HES1* promoter by cotransfecting a *HES1*-luciferase reporter plasmid and a plasmid expressing NICD, which acts as the transactivator of the *HES1* promoter (3, 10, 18, 19, 44), together with either GFP or GFP-Rbm15 expression plasmid. As seen in Fig. 5B, Rbm15 has a dose-dependent inhibitory effect on NICD-induced activation of the *HES1* promoter. In addition, Rbm15 also inhibits NICD-induced *HES1* promoter activity in HeLa cells (data not shown).

In contrast, when we performed analogous studies with hematopoietic cells, we observed the opposite effect. Rbm15 enhances NICD-induced *HES1* promoter activity in 32DWT18 cells in a dose-dependent manner (Fig. 5C). Analogous results were obtained with the HEL and promyelocytic (NB4) cell lines (data not shown). Therefore, the effect of Rbm15 on NICD-induced *HES1* promoter activity is cell type dependent, with an inhibitory effect in nonhematopoietic CHO and HeLa cells and a dramatic enhancing effect in three different hematopoietic cell lines. This result was particularly surprising given the known inhibitory effect of SHARP on transcription (see Discussion). In the absence of exogenous NICD, GFP-Rbm15 has no effect on *HES1* promoter activity in hematopoietic or nonhematopoietic cells, consistent with the lack of Notch activity in these cells.

Rbm15 binds to RBPJκ. To test whether Rbm15 interacts with RBPJκ, as has been shown previously for the fellow spen family member SHARP, coimmunoprecipitation experiments were performed using nuclear extracts of CHO cells that had been transfected with expression plasmids for RBPJκ and either GFP or GFP-Rbm15. As shown in Fig. 6A, immunoprecipitation with an anti-RBPJκ antibody followed by Western blot analysis with anti-GFP antibody revealed that RBPJκ binds to GFP-Rbm15 but not to GFP alone. Reciprocal experiments in which we used anti-GFP for immunoprecipitation and probed with anti-RBPJκ confirmed that GFP-Rbm15 binds to RBPJκ and that GFP does not (Fig. 6C). In order to determine which domain of Rbm15 is necessary for binding to RBPJκ, several truncation mutants of Rbm15 were tested for binding to RBPJκ (Fig. 6B). An N-terminal polypeptide of 608 aa (called N/Rbm15) was able to bind to RBPJκ, but a C-terminal 327-aa polypeptide (called C/Rbm15) was not (Fig.

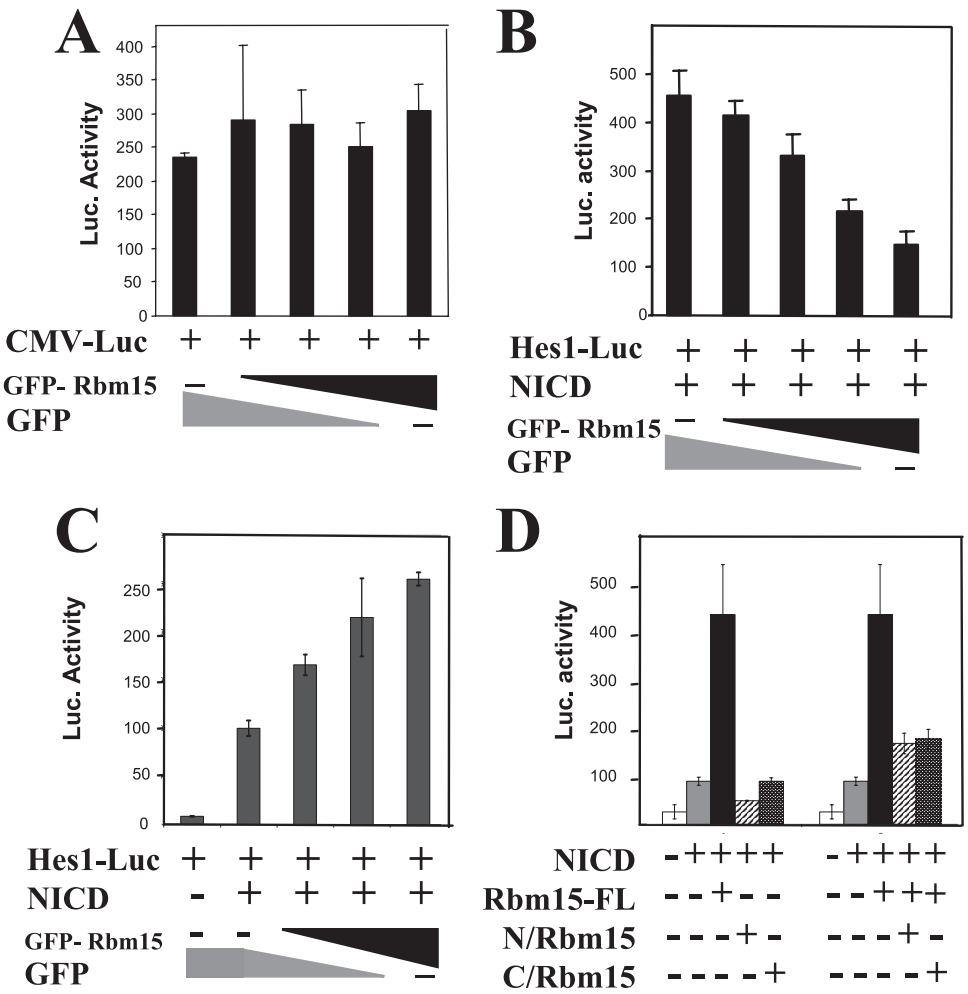

FIG. 5. Effect of Rbm15 on Notch-induced *HES1* promoter activity is cell type dependent. (A) CHO cells were cotransfected with CMV-Luc along with differing amounts of the GFP-Rbm15 expression plasmid as indicated by the dark black wedge. A GFP expression plasmid was used to maintain a constant DNA amount as indicated by the gray wedge. Data are presented as means ± standard deviations of luciferase activity from triplicate samples from one representative experiment of three that gave similar data. (B) Hes-1-Luc was used as the reporter plasmid, which is activated by NICD via its binding to RBPJκ on the Hes-1 promoter. As in panel A, different amounts of GFP-Rbm15 or GFP expression plasmid were cotransfected into CHO cells with the Hes-Luc and NICD expression plasmids as indicated. (C) 32DWT18 cells were transfected with Hes-Luc and NICD expression plasmids as indicated plus different amounts of GFP and/or GPP-Rbm15 expression plasmids as indicated. Note that a constant amount of DNA was included in every transfection. (D) Relative luciferase activity in 32DWT18 cells transfected as before with Hes-Luc (all lanes), NICD expression plasmid, and plasmids encoding various fragments of Rbm15. Plasmid names are as indicated in Fig. 6B.

6C). Further mapping was performed on the N-terminal portion of Rbm15, and we show that a fragment containing only the N-terminal 198 aa of the protein (Rbm15-F4) is adequate for binding RBPJκ (Fig. 6D).

Full-length Rbm15 is required for stimulation of NICD-induced *HES1* promoter activity. We next sought to determine the domains of Rbm15 required for enhancement of NICD-induced *HES1*-Luc activity in 32DWT18 cells. Only full-length Rbm15 showed this effect (Fig. 5D). Neither the N/Rbm15 nor the C/Rbm15 polypeptide alone had any effect on NICD-induced luciferase activity, suggesting that domains throughout the protein are required for this response. Similarly, the 198-aa N-terminal fragment of Rbm15 (Rbm15-F4) did not affect NICD-induced *HES1* promoter activity. Since N/Rbm15 can bind to RBP-Jκ but does not activate *HES1* promoter activity, we hypothesized that this fragment may interfere with the activity of full-length Rbm15. We tested this by cotransfecting N/Rbm15 along with the full-length Rbm15, NICD, and *HES1*-Luc plasmids (Fig. 5D). N/Rbm15 partially inhibits the enhancement of *HES1* promoter activity by FL Rbm15. Consistent with the need for full-length Rbm15 to enhance *HES1*-Luc activity, C/Rbm15 also inhibits the activity of full-length Rbm15 (Fig. 5D). Thus, both the N- and C-terminal segments have a dominant negative effect on full-length Rbm15.

DISCUSSION

The data presented here demonstrate that the murine homolog of human RBM15, the fusion partner of MKL1 in the AML-M7 t(1;22) translocation, plays a role in normal myelo-

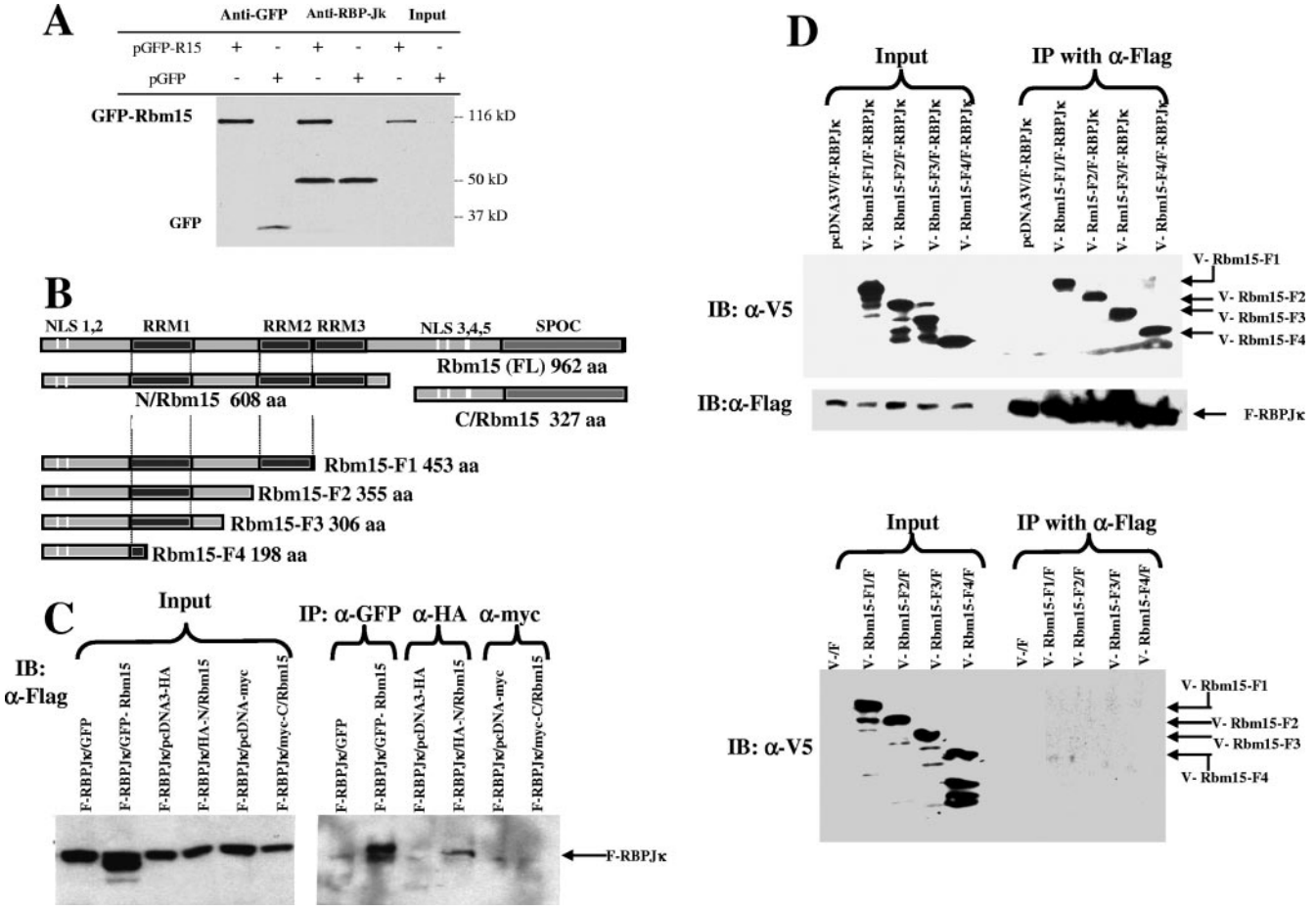

FIG. 6. Rbm15 coimmunoprecipitates with RBPJκ. (A) CHO cells were cotransfected with expression plasmids for either GFP or GFP-Rbm15, as indicated, plus expression plasmids for RBPJκ (all lanes). Nuclear extracts were immunoprecipitated with either anti-GFP (lanes 1 and 2) or anti-RBPJκ (lanes 3 and 4) and probed by Western analysis using anti-GFP. Lanes 5 and 6 show unmanipulated input. Bands representing the GFP-Rbm15 fusion protein and GFP are indicated. The band of approximately 60 kDa in lanes 3 and 4 likely represents the anti-RBPJκ antibody. (B) Schematic representation of Rbm15 truncations tested. The full-length (FL) mouse Rbm15 protein contains 962 aa. RNA recognition motifs (RRM) are located at aa 178 to 247, 374 to 446, and 455 to 524. The conserved SPOC domain is located at the C terminus from aa 778 to 957. Nuclear localization signal (NLS) sequences are predicted as shown. The pcDNA N/Rbm15 plasmid contains the 608-aa N-terminal fragment in frame with an HA tag. C/Rbm15 contains a 327-aa C-terminal fragment in frame with a myc tag. Rbm15-F1 through -F4 represent the truncated fragments from the N terminus with 453, 355, 306, and 198 aa, all fused in frame to a V5 tag. (C) Immunoprecipitation (IP) of Flag-tagged RBPJκ (F-RBPJκ) cotransfected with full-length Rbm15, empty pcDNA3, N/Rbm15, pcDNA-myc-tagged empty vector, and C/Rbm15, as indicated. Lysates were immunoprecipitated with anti-GFP, anti-HA, and anti-myc antibodies as shown, and the Western blot (IB) was probed with anti-Flag antibody. (D) Immunoprecipitation of the truncated Rbm15 fragments with anti-Flag antibody as indicated. The upper panel (right side) shows that the truncated Rbm15 polypeptides are all coimmunoprecipitated with RBPJκ (anti-Flag). The middle panel shows that the anti-Flag antibody precipitates the Flag-tagged RBPJκ protein. The bottom panel shows that the anti-Flag antibody in the presence of the Flag-tagged expression plasmid alone does not immunoprecipitate the truncated fragments of Rbm15.

poiesis. We show that Rbm15 is expressed at higher levels in hematopoietic progenitor cells than in more mature progeny, and inhibition of its expression by shRNA slows proliferation and promotes differentiation. Given our observation that Rbm15 expression stimulates the transcriptional activation of the *HES1* promoter by intracellular Notch in 32DWT18 and HEL cells, the proliferation/differentiation effects of Rbm15 may be mediated, at least in part, via its effect on Notch signaling. In support of this hypothesis, we also show that Rbm15 is a nuclear protein that binds to RBPJκ, the key downstream target of activated intracellular Notch.

Notch receptors and ligands are widely expressed in the hematopoietic system, including hematopoietic stem cells, as well as in the lymphoid, myeloid, and erythroid lineages (8, 24, 41). Several studies show that Notch facilitates bone marrow stem cell expansion and plays a role in the stem cell niche in vivo (11). In vitro activation of Notch in hematopoietic stem cells leads to increased proliferation and survival (13, 49). Notch signaling facilitates T-cell development and plays a role in biphenotypic fate decisions (24). The first mammalian homolog of *Drosophila* Notch was identified in a T-cell leukemia with aberrant constitutive Notch expression (12). Data regarding the effects of Notch on myeloid differentiation are inconsistent. In different situations, Notch has been shown to either inhibit (4, 36, 37) or enhance (42, 43) differentiation down the granulocytic and macrophage lineages. Consistent with publi-

cations showing that Notch signaling inhibits myeloid differentiation of 32D cells (4, 36, 37), our data show that Rbm15, which promotes Notch signaling in myeloid cells, has an inhibitory effect on myeloid differentiation. Similarly, we show that shRNA-mediated knockdown of Rbm15 leads to more rapid differentiation, suggesting that Notch is involved in inhibiting myeloid differentiation in our system. In preliminary studies, inhibition of Notch signaling by overexpression of a dominant negative form of mastermind (33) had only a small stimulatory effect on induction of Mac1 expression on 32DWT18 cell differentiation (data not shown). However, before dissection of the mechanisms involved, the relevance of these findings will first need to be confirmed using primary cells in follow-up studies.

The opposing effects of Rbm15 on NICD-induced *HES1* promoter activity in nonhematopoietic versus hematopoietic cells suggest that Rbm15 functions in a cell type-specific manner. This finding is reminiscent of the role of SKIP during Notch signaling. SKIP was identified as a component of a corepressor complex that represses RBPJκ transcriptional activity, but it was subsequently shown to bind to the Notch intracellular domain and to promote Notch activation (28, 51). It is possible that Rbm15 functions in a similar manner, associating with different cofactors in a cell-specific context that determines either an activation or a repression activity.

Since the Rbm15 homolog SHARP is thought of as a transcriptional repressor, we were surprised to observe a transcriptional activation activity of Rbm15 in hematopoietic cells. However, this disparity is in agreement with a recent study suggesting opposing roles for the RBM15 and SHARP *Drosophila* homologs, NITO and SPEN, respectively (20). In that study, although family members NITO and SPEN shared the common SPOC domain, they had opposing roles in *Drosophila* eye development (20). The authors proposed that there may be two classes of SPOC domain-containing proteins: large proteins such as SHARP and spen, which inhibit transcription, and small proteins such as Rbm15 and NITO, which have the opposite effect. This hypothesis is consistent with our data. Whether, like RBPJκ (38) and SKIP (51), there is competition between coactivators and corepressors for binding to the SPOC domain is not yet known.

We report that Rbm15 interacts via its N terminus (aa 1 to 198) with RBPJκ. Protein alignments and structural domain predictions show little homology with known RBPJκ interaction domains of other proteins, such as SHARP (38), the RTA protein of the Kaposi's sarcoma-associated herpesvirus (29), the Epstein-Barr virus nuclear antigens 2 and 3 (16), and the Notch1 RAM domain (23). The low sequence similarity among these domains probably reflects varied binding sites on RBPJκ. Differential binding of Rbm15 and SHARP to RBPJκ may underlie the functional differences between these two proteins of the same family.

AML, like other hematological malignancies, arises from an accumulation of mutations in hematopoietic stem and/or progenitor cells (6, 39, 40). Perhaps a clue as to the function of Rbm15 in hematopoiesis can be found by studying other genetic mutations that contribute to the genesis of AML-M7. In patients with Down syndrome who develop AML-M7 with trisomy 21, the 1;22 translocation is very rarely found; however, mutations in GATA1 that generate a truncated GATA1 protein are typically present (50). These GATA1 mutants retain their ability to bind DNA but lose transactivation ability (21). It is therefore possible that Rbm15 acts, in part, via inhibition of GATA1 activity, which is essential for normal erythroid and megakaryocytic development (46, 48). Moreover, interaction between Notch signaling and GATA1 transcriptional activity was demonstrated by the suppression of GATA1 activity by Notch-induced HES1 expression (17). If RBM15 normally inhibits hematopoietic differentiation, the involvement of RBM15 in the leukemia-associated RBM15-MKL1 fusion protein could possibly contribute to leukemogenesis by maintaining megakaryoblasts in an undifferentiated, proliferative state. Additional studies using RBM15, MKL1, and the RBM15-MKL1 fusion protein in erythromegakaryocytic progenitors will be required to more fully elucidate the role of the fusion protein in the development and/or maintenance of megakaryoblastic leukemia.

ACKNOWLEDGMENTS

This work was supported by NIH grants HL63357, DK0724429, and DK053037 and by St. Jude Cancer Center CORE grant CA21765 (to C.N. and S.W.M.); the Children's Leukemia Research Association, Inc.; the Leukemia Lymphoma Foundation; and the American Lebanese Syrian Associated Charities, St. Jude Children's Research Hospital.

We thank Yuying Ling for generously providing the Flag-RBPJκ expression plasmid; Warren Pear for the MAML retroviral expression plasmid; Xiaoli Cui for excellent experimental assistance; Michael Hodsdon for protein structure analysis; and Justin Cohen, Jiankan Guo, and Robert Harris for many helpful discussions.

REFERENCES

1. **Ballerini, P., A. Blaise, T. Mercher, B. Pellegrino, C. Perot, J. van den Akker, E. Gatbois, M. Adam, L. Douay, R. Berger, O. Bernard, and J. Landman-Parker.** 2003. A novel real-time RT-PCR assay for quantification of OTT-MAL fusion transcript reliable for diagnosis of t(1;22) and minimal residual disease (MRD) detection. Leukemia **17:**1193–1196.
2. **Baruchel, A., M. T. Daniel, G. Schaison, and R. Berger.** 1991. Nonrandom t(1;22)(p12-p13;q13) in acute megakaryocytic malignant proliferation. Cancer Genet. Cytogenet. **54:**239–243.
3. **Beatus, P., J. Lundkvist, C. Oberg, and U. Lendahl.** 1999. The notch 3 intracellular domain represses notch 1-mediated activation through Hairy/Enhancer of split (HES) promoters. Development **126:**3925–3935.
4. **Bigas, A., D. I. Martin, and L. A. Milner.** 1998. Notch1 and Notch2 inhibit myeloid differentiation in response to different cytokines. Mol. Cell. Biol. **18:**2324–2333.
5. **Carroll, A., C. Civin, N. Schneider, G. Dahl, A. Pappo, P. Bowman, A. Emami, S. Gross, C. Alvarado, C. Phillips, et al.** 1991. The t(1;22) (p13;q13) is nonrandom and restricted to infants with acute megakaryoblastic leukemia. Blood **78:**748–752.
6. **Charames, G. S., and B. Bapat.** 2003. Genomic instability and cancer. Curr. Mol. Med. **3:**589–596.
7. **Chen, F., and I. Rebay.** 2000. split ends, a new component of the Drosophila EGF receptor pathway, regulates development of midline glial cells. Curr. Biol. **10:**943–946.
8. **de Pooter, R. F., T. M. Schmitt, J. L. de la Pompa, Y. Fujiwara, S. H. Orkin, and J. C. Zuniga-Pflucker.** 2006. Notch signaling requires GATA-2 to inhibit myelopoiesis from embryonic stem cells and primary hemopoietic progenitors. J. Immunol. **176:**5267–5275.
9. **Du, K. L., M. Chen, J. Li, J. J. Lepore, P. Mericko, and M. S. Parmacek.** 2004. Megakaryoblastic leukemia factor-1 transduces cytoskeletal signals and induces smooth muscle cell differentiation from undifferentiated embryonic stem cells. J. Biol. Chem. **279:**17578–17586.
10. **Dumortier, A., R. Jeannet, P. Kirstetter, E. Kleinmann, M. Sellars, N. R. dos Santos, C. Thibault, J. Barths, J. Ghysdael, J. A. Punt, P. Kastner, and S. Chan.** 2006. Notch activation is an early and critical event during T-cell leukemogenesis in Ikaros-deficient mice. Mol. Cell. Biol. **26:**209–220.
11. **Duncan, A. W., F. M. Rattis, L. N. DiMascio, K. L. Congdon, G. Pazianos, C. Zhao, K. Yoon, J. M. Cook, K. Willert, N. Gaiano, and T. Reya.** 2005. Integration of Notch and Wnt signaling in hematopoietic stem cell maintenance. Nat. Immunol. **6:**314–322.
12. **Ellisen, L. W., J. Bird, D. C. West, A. L. Soreng, T. C. Reynolds, S. D. Smith, and J. Sklar.** 1991. TAN-1, the human homolog of the Drosophila notch

gene, is broken by chromosomal translocations in T lymphoblastic neoplasms. Cell **66:**649–661.
13. **Evans, C. J., V. Hartenstein, and U. Banerjee.** 2003. Thicker than blood: conserved mechanisms in Drosophila and vertebrate hematopoiesis. Dev. Cell **5:**673–690.
14. **Ge, Y., T. L. Jensen, M. L. Stout, R. M. Flatley, P. J. Grohar, Y. Ravindranath, L. H. Matherly, and J. W. Taub.** 2004. The role of cytidine deaminase and GATA1 mutations in the increased cytosine arabinoside sensitivity of Down syndrome myeloblasts and leukemia cell lines. Cancer Res. **64:**728–735.
15. **Hsiao, H. H., M. Y. Yang, Y. C. Liu, H. P. Hsiao, S. B. Tseng, M. C. Chao, T. C. Liu, and S. F. Lin.** 2005. RBM15-MKL1 (OTT-MAL) fusion transcript in an adult acute myeloid leukemia patient. Am. J. Hematol. **79:**43–45.
16. **Hsieh, J. J., and S. D. Hayward.** 1995. Masking of the CBF1/RBPJ kappa transcriptional repression domain by Epstein-Barr virus EBNA2. Science **268:**560–563.
17. **Ishiko, E., I. Matsumura, S. Ezoe, K. Gale, J. Ishiko, Y. Satoh, H. Tanaka, H. Shibayama, M. Mizuki, T. Era, T. Enver, and Y. Kanakura.** 2005. Notch signals inhibit the development of erythroid/megakaryocytic cells by suppressing GATA-1 activity through the induction of HES1. J. Biol. Chem. **280:**4929–4939.
18. **Jarriault, S., C. Brou, F. Logeat, E. H. Schroeter, R. Kopan, and A. Israel.** 1995. Signalling downstream of activated mammalian Notch. Nature **377:** 355–358.
19. **Jarriault, S., O. Le Bail, E. Hirsinger, O. Pourquie, F. Logeat, C. F. Strong, C. Brou, N. G. Seidah, and A. Israel.** 1998. Delta-1 activation of notch-1 signaling results in HES-1 transactivation. Mol. Cell. Biol. **18:**7423–7431.
20. **Jemc, J., and I. Rebay.** 2006. Characterization of the split ends-like gene spenito reveals functional antagonism between SPOC family members during Drosophila eye development. Genetics **173:**279–286.
21. **Kawaguchi, H., J. K. Hitzler, Z. Ma, and S. W. Morris.** 2005. RBM15 and MKL1 mutational screening in megakaryoblastic leukemia cell lines and clinical samples. Leukemia **19:**1492–1494.
22. **Khanna-Gupta, A., T. Zibello, H. Sun, J. Lekstrom-Himes, and N. Berliner.** 2001. C/EBP epsilon mediates myeloid differentiation and is regulated by the CCAAT displacement protein (CDP/cut). Proc. Natl. Acad. Sci. USA **98:** 8000–8005.
23. **Kovall, R. A., and W. A. Hendrickson.** 2004. Crystal structure of the nuclear effector of Notch signaling, CSL, bound to DNA. EMBO J. **23:**3441–3451.
24. **Krause, D. S.** 2002. Regulation of hematopoietic stem cell fate. Oncogene **21:**3262–3269.
25. **Kuang, B., S. C. Wu, Y. Shin, L. Luo, and P. Kolodziej.** 2000. split ends encodes large nuclear proteins that regulate neuronal cell fate and axon extension in the Drosophila embryo. Development **127:**1517–1529.
26. **Kuroda, K., H. Han, S. Tani, K. Tanigaki, T. Tun, T. Furukawa, Y. Taniguchi, H. Kurooka, Y. Hamada, S. Toyokuni, and T. Honjo.** 2003. Regulation of marginal zone B cell development by MINT, a suppressor of Notch/RBP-J signaling pathway. Immunity **18:**301–312.
27. **Kuwahara, K., T. Barrientos, G. C. Pipes, S. Li, and E. N. Olson.** 2005. Muscle-specific signaling mechanism that links actin dynamics to serum response factor. Mol. Cell. Biol. **25:**3173–3181.
28. **Leong, G. M., N. Subramaniam, L. L. Issa, J. B. Barry, T. Kino, P. H. Driggers, M. J. Hayman, J. A. Eisman, and E. M. Gardiner.** 2004. Ski-interacting protein, a bifunctional nuclear receptor coregulator that interacts with N-CoR/SMRT and p300. Biochem. Biophys. Res. Commun. **315:**1070–1076.
29. **Liang, Y., J. Chang, S. J. Lynch, D. M. Lukac, and D. Ganem.** 2002. The lytic switch protein of KSHV activates gene expression via functional interaction with RBP-Jkappa (CSL), the target of the Notch signaling pathway. Genes Dev. **16:**1977–1989.
30. **Lion, T., O. A. Haas, J. Harbott, E. Bannier, J. Ritterbach, M. Jankovic, F. M. Fink, A. Stojimirovic, J. Herrmann, H. J. Riehm, et al.** 1992. The translocation t(1;22)(p13;q13) is a nonrandom marker specifically associated with acute megakaryocytic leukemia in young children. Blood **79:**3325–3330.
31. **Ma, Z., S. W. Morris, V. Valentine, M. Li, J. A. Herbrick, X. Cui, D. Bouman, Y. Li, P. K. Mehta, D. Nizetic, Y. Kaneko, G. C. Chan, L. C. Chan, J. Squire, S. W. Scherer, and J. K. Hitzler.** 2001. Fusion of two novel genes, RBM15 and MKL1, in the t(1;22)(p13;q13) of acute megakaryoblastic leukemia. Nat. Genet. **28:**220–221.
32. **Magalhaes, I. Q., A. Splendore, M. Emerenciano, A. Figueiredo, I. Ferrari, and M. S. Pombo-de-Oliveira.** 2006. GATA1 mutations in acute leukemia in children with Down syndrome. Cancer Genet. Cytogenet **166:**112–116.
33. **Maillard, I., A. P. Weng, A. C. Carpenter, C. G. Rodriguez, H. Sai, L. Xu, D. Allman, J. C. Aster, and W. S. Pear.** 2004. Mastermind critically regulates Notch-mediated lymphoid cell fate decisions. Blood **104:**1696–1702.
34. **Mercher, T., M. Busson-Le Coniat, F. N. Khac, P. Ballerini, M. Mauchauffe, H. Bui, B. Pellegrino, I. Radford, F. Valensi, F. Mugneret, N. Dastugue, O. A. Bernard, and R. Berger.** 2002. Recurrence of OTT-MAL fusion in t(1;22) of infant AML-M7. Genes Chromosomes Cancer **33:**22–28.
35. **Mercher, T., M. B. Coniat, R. Monni, M. Mauchauffe, F. N. Khac, L. Gressin, F. Mugneret, T. Leblanc, N. Dastugue, R. Berger, and O. A. Bernard.** 2001. Involvement of a human gene related to the Drosophila spen gene in the recurrent t(1;22) translocation of acute megakaryocytic leukemia. Proc. Natl. Acad. Sci. USA. **98:**5776–5779.
36. **Milner, L. A., and A. Bigas.** 1999. Notch as a mediator of cell fate determination in hematopoiesis: evidence and speculation. Blood **93:**2431–2448.
37. **Milner, L. A., A. Bigas, R. Kopan, C. Brashem-Stein, I. D. Bernstein, and D. I. K. Martin.** 1996. Inhibition of granuloctic differentiation by mNotch1. Proc. Natl. Acad. Sci. USA **93:**13014–13019.
38. **Oswald, F., U. Kostezka, K. Astrahantseff, S. Bourteele, K. Dillinger, U. Zechner, L. Ludwig, M. Wilda, H. Hameister, W. Knochel, S. Liptay, and R. M. Schmid.** 2002. SHARP is a novel component of the Notch/RBP-Jkappa signalling pathway. EMBO J. **21:**5417–5426.
39. **Pavlova, S., J. Mayer, H. Koukalova, and J. Smardova.** 2003. High frequency of temperature-sensitive mutations of p53 tumor suppressor in acute myeloid leukemia revealed by functional assay in yeast. Int. J. Oncol. **23:**121–131.
40. **Pihan, G., and S. J. Doxsey.** 2003. Mutations and aneuploidy: co-conspirators in cancer? Cancer Cell **4:**89–94.
41. **Radtke, F., A. Wilson, S. J. Mancini, and H. R. MacDonald.** 2004. Notch regulation of lymphocyte development and function. Nat. Immunol. **5:**247–253.
42. **Schroeder, T., and U. Just.** 2000. Notch signalling via RBP-J promotes myeloid differentiation. EMBO J. **19:**2558–2568.
43. **Schroeder, T., H. Kohlhof, N. Rieber, and U. Just.** 2003. Notch signaling induces multilineage myeloid differentiation and up-regulates PU.1 expression. J. Immunol. **170:**5538–5548.
44. **Schroeter, E. H., J. A. Kisslinger, and R. Kopan.** 1998. Notch-1 signalling requires ligand-induced proteolytic release of intracellular domain. Nature **393:**382–386.
45. **Shi, Y., M. Downes, W. Xie, H. Y. Kao, P. Ordentlich, C. C. Tsai, M. Hon, and R. M. Evans.** 2001. Sharp, an inducible cofactor that integrates nuclear receptor repression and activation. Genes Dev. **15:**1140–1151.
46. **Shivdasani, R. A.** 1997. Stem cell transcription factors. Hematol. Oncol. Clin. N. Am. **11:**1199–1206.
47. **Sierra, O. L., S. L. Cheng, A. P. Loewy, N. Charlton-Kachigian, and D. A. Towler.** 2004. MINT, the Msx2 interacting nuclear matrix target, enhances Runx2-dependent activation of the osteocalcin fibroblast growth factor response element. J. Biol. Chem. **279:**32913–32923.
48. **Stachura, D. L., S. T. Chou, and M. J. Weiss.** 2006. Early block to erythromegakaryocytic development conferred by loss of transcription factor GATA-1. Blood **107:**87–97.
49. **Vas, V., L. Szilagyi, K. Paloczi, and F. Uher.** 2004. Soluble Jagged-1 is able to inhibit the function of its multivalent form to induce hematopoietic stem cell self-renewal in a surrogate in vitro assay. J. Leukoc. Biol. **75:**714–720.
50. **Wechsler, J., M. Greene, M. A. McDevitt, J. Anastasi, J. E. Karp, M. M. Le Beau, and J. D. Crispino.** 2002. Acquired mutations in GATA1 in the megakaryoblastic leukemia of Down syndrome. Nat. Genet. **32:**148–152.
51. **Zhou, S., M. Fujimuro, J. J. Hsieh, L. Chen, A. Miyamoto, G. Weinmaster, and S. D. Hayward.** 2000. SKIP, a CBF1-associated protein, interacts with the ankyrin repeat domain of NotchIC To facilitate NotchIC function. Mol. Cell. Biol. **20:**2400–2410.